Fission yeast mto2p regulates microtubule nucleation by the centrosomin-related protein mto1p

Molecular Biology of the Cell
Vol. 16, 3040–3051, June 2005

Fission Yeast mto2p Regulates Microtubule Nucleation by the Centrosomin-related Protein mto1p[V]

Itaru Samejima, Paula C. C. Lourenço,* Hilary A. Snaith, and Kenneth E. Sawin

Wellcome Trust Centre for Cell Biology, School of Biological Sciences, University of Edinburgh, Edinburgh EH9 3JR, United Kingdom

Submitted November 16, 2004; Revised January 3, 2005; Accepted January 5, 2005
Monitoring Editor: Trisha Davis

From an insertional mutagenesis screen, we isolated a novel gene, *mto2+*, involved in microtubule organization in fission yeast. *mto2Δ* strains are viable but exhibit defects in interphase microtubule nucleation and in formation of the postanaphase microtubule array at the end of mitosis. The *mto2Δ* defects represent a subset of the defects displayed by cells deleted for *mto1+* (also known as *mod20+* and *mbo1+*), a centrosomin-related protein required to recruit the γ-tubulin complex to cytoplasmic microtubule-organizing centers (MTOCs). We show that mto2p colocalizes with mto1p at MTOCs throughout the cell cycle and that mto1p and mto2p coimmunoprecipitate from cytoplasmic extracts. In vitro studies suggest that mto2p binds directly to mto1p. In *mto2Δ* mutants, although some aspects of mto1p localization are perturbed, mto1p can still localize to spindle pole bodies and the cell division site and to "satellite" particles on interphase microtubules. In *mto1Δ* mutants, localization of mto2p to all of these MTOCs is strongly reduced or absent. We also find that in *mto2Δ* mutants, cytoplasmic forms of the γ-tubulin complex are mislocalized, and the γ-tubulin complex no longer coimmunoprecipitates with mto1p from cell extracts. These experiments establish mto2p as a major regulator of mto1p-mediated microtubule nucleation by the γ-tubulin complex.

INTRODUCTION

The γ-tubulin complex is a large, conserved multisubunit protein complex involved in microtubule nucleation in eukaryotic cells (Stearns and Kirschner, 1994; Zheng *et al*., 1995; for reviews, see Gunawardane *et al*., 2000; Oakley, 2000; Schiebel, 2000; Job *et al*., 2003). In a variety of cell types, the γ-tubulin complex is found both localized to microtubule-organizing centers (MTOCs) and also in significant levels in cytoplasmic pools. Although much of the characterization of γ-tubulin function has involved work on soluble complexes, most MTOCs in vivo are associated with largely insoluble compartments or subcellular organelles, and as a result we currently understand very little of the mechanisms controlling the intracellular localization and activity of the γ-tubulin complex and how these mechanisms might be regulated. Recently, a small number of proteins have been identified that may interact with the γ-tubulin complex and recruit it to structures such as the centrosome, the Golgi apparatus, or other MTOCs (Takahashi *et al*., 2002; Terada *et al*., 2003; Kawaguchi and Zheng, 2004; Rios *et al*., 2004; Sawin *et al*., 2004; Thompson *et al*., 2004; Venkatram *et al*., 2004; Zimmerman *et al*., 2004a,b). However, in this area much still remains to be learned.

The fission yeast *Schizosaccharomyces pombe* has recently become a useful model system for understanding microtubule nucleation and dynamics. Three distinct patterns of microtubule nucleation take place during the mitotic cell cycle in fission yeast (Hagan, 1998). During interphase, dynamic microtubules tend to run along the long axis of the cylindrically shaped cells and terminate at cell tips. These microtubules are nucleated from cytoplasmic interphase MTOCs (iMTOCs) in the middle of the cell that may be associated with the nuclear envelope or with microtubule bundles themselves (Drummond and Cross, 2000; Tran *et al*., 2001; Sawin *et al*., 2004; Zimmerman *et al*., 2004a). Nucleation sites on the surface of the nucleus are easily recognized in microtubule regrowth experiments after microtubule depolymerization, but whether they exist in the same form during steady-state growth is unclear. By contrast, although de novo nucleation of microtubules from microtubule bundles has not yet been directly observed in growing cells, components of the γ-tubulin complex are seen not only at the spindle pole body (SPB, the yeast centrosome equivalent) but also in the form of small satellite particles moving along microtubules (Sawin *et al*., 2004; Zimmerman *et al*., 2004a). Against this background of incomplete understanding, in this work we apply the term "iMTOC" somewhat freely, both to nuclear surface nucleation sites and to the aforesaid microtubule-associated particles. During mitosis, duplicated SPBs nucleate an intranuclear mitotic spindle, as well as cytoplasmic astral microtubules, which may help to position the spindle and/or coordinate mitotic progression with cytokinesis (Gachet *et al*., 2001; Oliferenko and Balasubramanian, 2002; Gachet *et al*., 2004). At the end of mitosis, a specialized microtubule structure, termed the postanaphase array (PAA), is nucleated from an equatorial MTOC

This article was published online ahead of print in *MBC in Press* (http://www.molbiolcell.org/cgi/doi/10.1091/mbc.E04–11–1003) on January 19, 2005.

[V] The online version of this article contains supplemental material at *MBC Online* (http://www.molbiolcell.org).

* Present address: National CJD Surveillance Unit, Western General Hospital, Crewe Rd., Edinburgh EH4 2XU, United Kingdom.

Address correspondence to: Kenneth E. Sawin (ken.sawin@ed.ac.uk).

Abbreviations: eMTOC, equatorial microtubule-organizing center; iMTOC, interphase microtubule-organizing center; PAA, postanaphase array; SPB, spindle pole body.

(eMTOC) at the cell division site (Heitz *et al*., 2001; Pardo and Nurse, 2003).

There is good evidence that γ-tubulin plays a role in microtubule nucleation at all fission yeast MTOCs (Horio *et al*., 1991; Paluh *et al*., 2000; Heitz *et al*., 2001; Sawin *et al*., 2004; Venkatram *et al*., 2004; Zimmerman *et al*., 2004a). Thus far, nearly all of the subunits of the higher eukaryotic γ-tubulin complex have been identified in fission yeast (Horio *et al*., 1991; Stearns *et al*., 1991; Vardy and Toda, 2000; Fujita *et al*., 2002; Venkatram *et al*., 2004), and recent efforts have begun to identify fission yeast proteins regulating γ-tubulin function. The nonessential protein mod20p/mbo1p seems to play a particularly important role in γ-tubulin complex-mediated microtubule nucleation (Sawin *et al*., 2004; Venkatram *et al*., 2004). To establish a common nomenclature, from hereon in this article we refer to mod20p/mbo1p as *m*icro*t*ubule *o*rganizer 1 (mto1p). In *mto1*Δ mutants, new microtubule nucleation by iMTOCs is profoundly crippled, such that only the SPB is (poorly) active for microtubule nucleation. In addition, during mitosis, *mto1*Δ mutants fail to nucleate cytoplasmic astral microtubules, although the assembly of the intranuclear mitotic spindle seems to be normal. Moreover, at the end of mitosis, when wild-type cells form a PAA, *mto1*Δ mutants fail to nucleate any microtubules from the cell division site. The role of mto1p in these various manifestations of spatially restricted microtubule nucleation seems to be to recruit the γ-tubulin complex to MTOCs, as components of the γ-tubulin complex are coimmunoprecipitated with mto1p, and in *mto1*Δ cells, the γ-tubulin complex is specifically absent from the sites at which microtubule nucleation should but does not occur.

Potential homologues of mto1p are found in fungi and in higher eukaryotes. These are all large proteins, with extensive regions of predicted α-helical coiled-coil, and they share in their amino-terminus a roughly 60-amino acid region of limited sequence conservation. Some of these proteins, such as *Aspergillus nidulans* apsB and *Drosophila* centrosomin (*cnn*), have been characterized functionally (Suelmann *et al*., 1998; Megraw *et al*., 1999; Terada *et al*., 2003), and this analysis is consistent with the proposed function of mto1p. Other proteins, such as human myomegalin/PDE4DIP or CDK5RAP2, are to date only little characterized (Ching *et al*., 2000; Verde *et al*., 2001; Andersen *et al*., 2003), but they are likely, even on the basis of limited analysis, to be equally interesting. Amino acid sequence analysis also suggests that in some organisms, mto1p-like proteins may exist as pairs of paralogs. For example, in fission yeast, the putative mto1p paralog pcp1p, which may be orthologous to budding yeast Spc110p (Knop and Schiebel, 1998; Flory *et al*., 2002), has been hypothesized to be responsible for intranuclear mitotic spindle microtubule nucleation, which is independent of mto1p (Sawin *et al*., 2004; Venkatram *et al*., 2004).

From this perspective, a deeper understanding of how mto1p localization and activity are regulated should provide further insights into the mechanisms controlling microtubule nucleation by the γ-tubulin complex in fission yeast. Here, we describe a novel nonessential gene, *mto2*+, which is involved in mto1p-mediated microtubule nucleation. Mto2p is physically associated with mto1p and colocalizes with mto1p throughout the cell cycle. Interestingly, *mto2*Δ mutants display a subset of the microtubule-nucleation–defective phenotypes seen in *mto1*Δ mutants. Collectively, our results suggest that mto2p promotes the ability of mto1p to recruit the γ-tubulin complex to a subset of MTOCs away from the SPB.

MATERIALS AND METHODS

Yeast Strain Construction and Growth Conditions

Standard yeast genetic techniques were used throughout (Moreno *et al*., 1991; Alfa *et al*., 1993). Insertional mutagenesis was performed as described previously (Snaith and Sawin, 2003). Deletion and tagging of genes at both N and C termini was achieved using polymerase chain reaction (PCR)-based targeting methods (Bahler *et al*., 1998), and deletions and tagging were confirmed by PCR and Western blotting as appropriate. See Table 1 for a list of strains used. The cyan fluorescent protein (CFP)-atb2 plasmid pRL72 (Glynn *et al*., 2001) was used to transform strains for the experiments shown in Figure 7. Growth conditions were as described previously (Moreno *et al*., 1991), except that sodium glutamate was used as nitrogen source for minimal medium. Although this is unrelated to *mto2*+ function per se, we note for interested investigators that the *mto2*+ locus is closely linked (distance ~10 kb) to *alp6*+, an essential component of the γ-tubulin complex (Vardy and Toda, 2000).

Antibodies

Antibodies to mto2p were raised in sheep against recombinant glutathione *S*-transferase (GST)-mto2p purified from *Escherichia coli*. Anti-mto2p antibody was affinity purified from serum by using standard methods (Sawin *et al*., 1992). First, anti-GST antibodies were removed by passing serum through a column of GST coupled to Affigel (Bio-Rad, Hercules, CA) until all anti-GST reactivity was removed. Anti-mto2p antibodies were then affinity purified on a column of GST-mto2p coupled to Affigel and eluted at pH 3.0. The anti-mto1p polyclonal antibody and TAT1 anti-tubulin (Woods *et al*., 1989), 9E10 anti-myc (Evan *et al*., 1985), and GTU-88 anti-γ-tubulin (Sigma-Aldrich, St. Louis, MO) monoclonal antibodies were used as described previously (Sawin *et al*., 2004). Secondary antibodies were Alexa labeled (Molecular Probes, Eugene, OR) for immunofluorescence and horseradish peroxidase labeled (Amersham Biosciences, Piscataway, NJ; and Sigma-Aldrich) for Western blotting.

Immunofluorescence and Physiology Experiments

For anti-tubulin and anti-mto1p immunofluorescence, cells were fixed in methanol at –70°C and processed exactly as described previously (Sawin and Nurse, 1998; Sawin *et al*., 2004).

Cell morphology assays after growth to stationary phase on YE5S agar plates were performed as described previously (Snaith and Sawin, 2003). Cells were washed off plates and fixed in 3% formaldehyde before imaging. Assays of microtubule regrowth after cold-shock were as described previously (Sawin *et al*., 2004). Exponentially growing cells were chilled in ice water bath for 30 min and transferred to a prewarmed flask and incubated at 32°C for the specified time before collection by filtration and fixation. Mitotic block-and-release experiments by using reversible cold-sensitive *nda3* mutants also were exactly as described previously (Sawin *et al*., 2004).

Biochemical Methods

For coimmunoprecipitation experiments of mto2p with mto1p, yeast cells were disrupted by bead-beating by using 0.5-mm zirconium beads in a buffer containing 50 mM Tris, pH 8.0, 150 mM NaCl, 1 mM EDTA, and 1 mM phenylmethylsulfonyl fluoride (PMSF). Cleared cell extract was incubated with anti-myc antibody (9E10) or affinity-purified anti-mto2p antibody for 30 min. Protein A- or protein G-Sepharose was added to the cell extract/antibody mixture and incubated for a further 30 min at 4°C. The Sepharose beads were washed four times with the buffer before being boiled in 2× SDS PAGE buffer and used for SDS-PAGE and Western blotting.

For coimmunoprecipitation experiments of mto1p with components of the γ-tubulin complex, frozen yeast cells were disrupted by grinding with a mortar and pestle. These and further manipulations were carried out exactly as described previously (Sawin *et al*., 2004).

A TnT T7 coupled in vitro transcription/translation kit (Promega, Madison, WI) was used to synthesize mto1p polypeptides for use in GST pull-down assays. GST-mto2p was expressed in *E. coli* BL21(DE3)pLysS and purified on glutathione (GSH)-Sepharose (Amersham Biosciences) following manufacturer's instructions. Truncated *mto1* genes were amplified by PCR from a plasmid template, and the resulting PCR products were used as the template for in vitro transcription/translation. All 5′ primers start with a common 40-base sequence (5′-CCGCGGGGCCCTAATACGACTCACTATAGGGAGAACCA-TG-3′, which contains T7 primer, Kozak sequence, and an initiation methionine codon) followed by the appropriate specific mto1 sequence. Fifteen microliters of a 50-μl reaction was incubated with GST-mto2p bound to GSH-Sepharose (Sigma-Aldrich) in 500 μl of GST binding buffer (50 mM Tris, pH 7.5, 100 mM NaCl, 1% Triton X-100, 10% glycerol, and 1 mM PMSF) at 4°C for 1 h. Beads were washed four times with the GST binding buffer before boiling in 2× SDS-PAGE buffer.

In Vivo Fluorescence Imaging

Single time-point and time-lapse imaging of green fluorescent protein (GFP)-, CFP-, and yellow fluorescent protein (YFP)-fusion proteins in fission yeast was essentially as described previously (Snaith and Sawin, 2003; Sawin *et al*.,

Table 1. Fission yeast strains used in this study

Strain no.	Genotype	Source
KS515	*h+ ade6-216 leu1-32 ura4-D18*	Laboratory stock
KS516	*h– ade6-210 leu1-32 ura4-D18*	Laboratory stock
KS819	*h+ mto1-GFP:kanMX6 ade6-216 leu1-32 ura4-D18*	Laboratory stock (Sawin *et al*., 2004)
KS968	*h+ mto2Δ::kanMX6 kanMX6 nmt41:GFP-atb2 ade6-216*	This study
KS976	*h– mto2Δ::kanMX6 ade6-216 leu1-32 ura4-D18*	This study
KS1014	*h– mto1Δ::kanMX6 mto2Δ::kanMX6 ade6-216 leu1-32 ura4-D18*	This study
KS1138	*h– alp4-3HA:kanMX6 ade6 his leu1-32 ura4-D18*	T. Toda (Vardy *et al*., 2000)
KS1158	*h– mto1Δ::kanMX6 ade6-210 leu1-32 ura4-D18*	Laboratory stock (Sawin *et al*., 2004)
KS1236	*h– kanMX6:nmt81:GFP-atb2 ade6-210 leu1-32 ura4-D18*	Laboratory stock (Sawin *et al*., 2004)
KS1238	*h– nda3-KM311 ade6-210 leu1-32 ura4-D18*	Laboratory stock (Hiraoka *et al*. 1984)
KS1368	*h+ alp4-GFP:kanMX6 ade6-216 leu1-32 ura4-D18*	T. Toda (Vardy *et al*., 2000)
KS1370	*h– alp4-3HA:kanMX6 ade6-216 leu1-32 ura4-D18*	This study
KS1389	*h– kanMX6:nmt81:GFP-mto1 ade6-210 leu1-32 ura4-D18*	This study
KS1407	*h– mto1-GFP:kanMX6 mto2Δ::kanMX6 ade6-216 leu1-32 ura4-D18*	This study
KS1408	*h+ mto1-GFP:kanMX6 mto2Δ::kanMX6 ade6-216 leu1-32 ura4-D18*	This study
KS1409	*h– mto2Δ::kanMX6 kanMX6:nmt81:GFP-atb2 ade6-216 leu1-32 ura4-D18*	This study
KS1431	*h– kanMX6:nmt81:GFP-mto1 mto2Δ::kanMX6 ade6-210 leu1-32 ura4-D18*	This study
KS1459	*h+ mto1Δ::kanMX6 mto2-GFP:kanMX6 ade6-216 leu1-32 ura4-D18*	This study
KS1478	*h– kanMX6:nmt41:GFP-mto2 ade6-210 leu1-32 ura4-D18*	This study
KS1507	*h+ mto1-13myc:kanMX6 ade6-216 leu1-32 ura4-D18*	Laboratory stock (Sawin *et al*., 2004)
KS1517	*h– alp4-3HA:kanMX6 mto1-13myc:kanMX6 ade6-216 leu1-32 ura4-D18*	Laboratory stock (Sawin *et al*., 2004)
KS1607	*h– mto2Δ::kanMX6 nda3-KM311 ade6-210 leu1-32 ura4-D18*	This study
KS1615	*h– mto1(1-285)-13myc:kanMX6*	This study
KS1616	*h– mto1(1-500)-13myc:kanMX6 ade6-210 leu1-32 ura4-D18*	This study
KS1617	*h– mto1(1-800)-13myc:kanMX6 ade6-210 leu1-32 ura4-D18*	This study
KS1619	*h– mto1(1-1051)-13myc:kanMX6 ade6-210 leu1-32 ura4-D18*	This study
KS1640	*h– mto1-13myc:kanMX6 mto2Δ::kanMX6 ade6-216 leu1-32 ura4-D18*	This study
KS1889	*h+ mto2-GFP:kanMX6 ade6-216 leu1-32 ura4-D18*	This study
KS2120	*h+ mto1-YFP:kanMX6 ade6-216 leu1-32 ura4-D18*	This study
KS2131	*h– kanMX6:nmt41:GFP-mto2 kanMX6:nmt81:mto1 ade6-210 leu1-32 ura4-D18*	This study
KS2156	*h– mto2-CFP:kanMX6 ade6-210 leu1-32 ura4-D18*	This study
KS2169	*h– mto1-13myc:kanMX6 mto2Δ::kanMX6 alp4-3HA:kanMX6 ade6-216 leu1-32 ura4-D18*	This study
KS2180	*h– mto1-YFP:kanMX6 mto2-CFP:kanMX6 ade6-216 leu1-32 ura4-D18*	This study
KS2220	*h+ mto1-YFP:kanMX6 mto2Δ::kanMX6 ade6-216 leu1-32 ura4-D18*	This study
KS2248	*h+ alp4-GFP:natMX6 ade6-216 leu1-32 ura4-D18*	This study
KS2258	*h+ alp4-GFP:natMX6 mto2Δ::kanMX6 ade6-216 leu1-32 ura4-D18*	This study

2004). Cells were mounted on medium-agarose pads before imaging and sealed with VALAP. Images were collected on a Nikon TE300 inverted microscope with automated filter and *z*-axis control, running MetaMorph software (Universal Imaging, Downingtown, PA). Appropriate neutral density filters were used to reduce photobleaching and photodamage. Some sequences were further deconvolved using Softworx (Applied Precision, Issaquah, WA).

RESULTS

Aberrant Cell Shape and Microtubule Organization in mto2 Mutants

From an insertional mutagenesis screen designed to identify genes regulating cell polarity in fission yeast (Snaith and Sawin, 2003), we isolated a mutant that produces a curved cell shape upon return to growth from stationary phase (Figure 1A). Sequencing of the disrupted gene showed it to be SPBC902.06, a previously uncharacterized open reading frame, which we have termed *mto2+*. Database searches did not reveal any obvious eukaryotic homologues of mto2p at the primary sequence level. Targeted deletion of the *mto2+* open reading frame yielded viable cells (*mto2*Δ) with a phenotype identical to the original disruption mutant, and the *mto2*Δ strain was used for all subsequent experiments.

The cell shape phenotype of *mto2*Δ mutants closely resembled that of deletion mutants of the recently characterized gene *mto1+* (Sawin and Snaith, 2004; Venkatram *et al*., 2004). Mto1p is required for microtubule nucleation from non-SPB sites within the cell as well as for the nucleation of cytoplasmic (but not intranuclear) microtubules from the SPB, and mto1p acts to recruit the γ-tubulin complex to these sites (Sawin and Snaith, 2004; Venkatram *et al*., 2004). We therefore examined both cell shape and microtubule organization in *mto2*Δ mutants relative to *mto1*Δ single mutants and to *mto1*Δ *mto2*Δ double mutants (Figure 1, A and B). Cell shape defects were not more severe in the double mutant relative to either single mutant, suggesting that mto1p and mto2p gene products may act in the same genetic pathway. Similar results also were obtained with regard to microtubule organization, in which both single and double mutants showed a range of microtubule defects normally not seen in wild-type cells, including fewer (and often thicker) microtubule bundles per cell and microtubules curving around cell tips.

We next examined the behavior of *mto2*Δ mutants in microtubule regrowth assays after a cold shock at 0°C. In these experiments, wild-type interphase cells rapidly renucleate microtubules from numerous independent sites in the cell middle, probably in contact with the nuclear surface, whereas *mto1*Δ mutants renucleate microtubules extremely slowly and then only from the SPB (Figure 2; Sawin *et al*., 2004). Comparing wild-type, *mto1*Δ, and *mto2*Δ cells in this assay, we found that *mto2*Δ mutants showed a phenotype distinct from both wild-type cells and *mto1*Δmutants. Al-

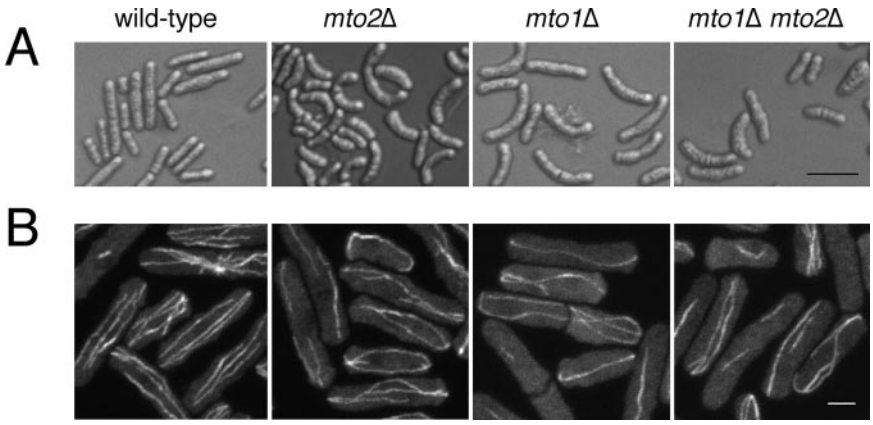

Figure 1. Phenotype of *mto2*Δ cells. (A) Morphology of wild-type and mutant cells 3 h after return to fresh medium from stationary phase. Only wild-type cells are straight. Bar, 10 μm. (B) Microtubule organization in wild-type and mutant cells, as shown by anti-tubulin immunofluorescent staining of asynchronous cultures. Note that mutants tend to have fewer microtubule bundles, and bundles often curve around cell tips. Bar, 2 μm.

though, as in *mto1*Δ mutants, microtubule nucleation in *mto2*Δ mutants was restricted to a single bundle growing from the SPB, the rate of regrowth was considerably faster in *mto2*Δ mutants, which reached a steady-state distribution ~10 min after warming, in contrast to 30–60 min for *mto1*Δ cells and ~4 min for wild-type cells (Figure 2). In these experiments, *mto1*Δ *mto2*Δ double mutants showed the strong defects characteristic of *mto1*Δ single mutants, further supporting the notion that mto1p and mto2p act in a common genetic pathway.

The defects in interphase microtubule nucleation observed in *mto2*Δ mutants in microtubule regrowth experi-

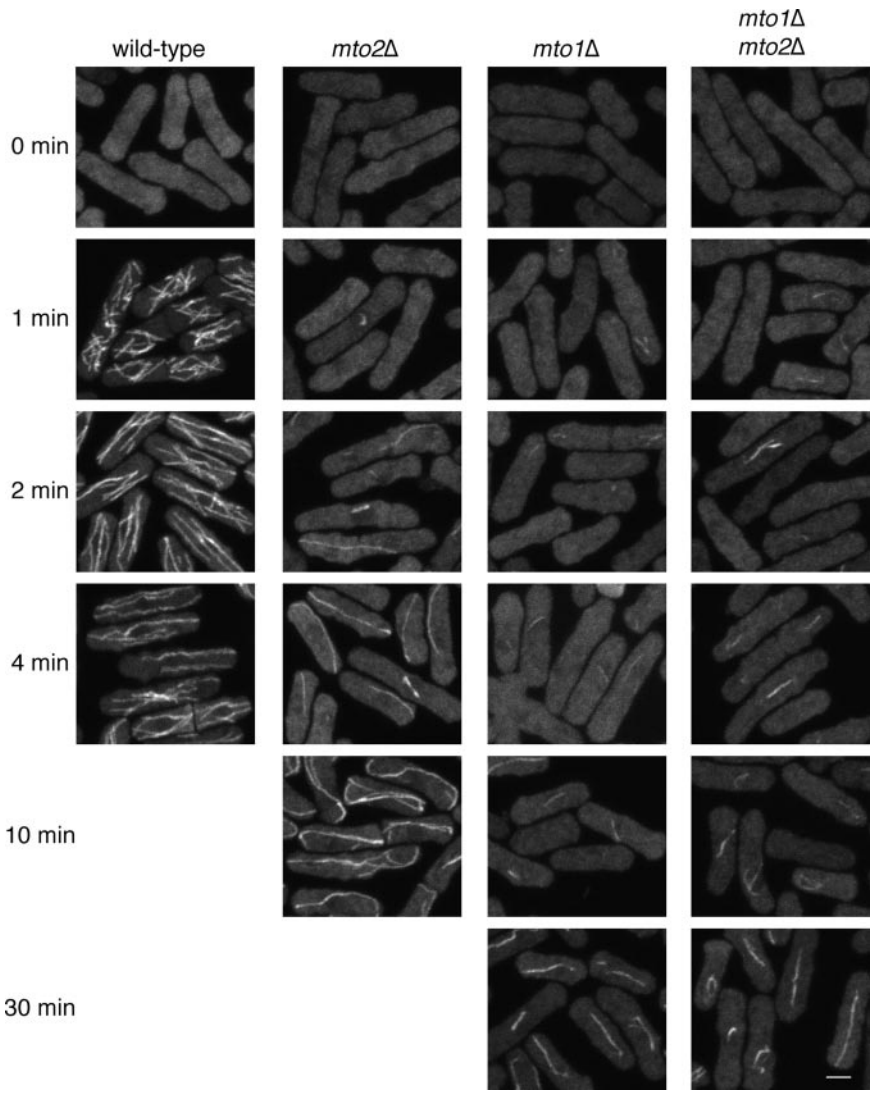

Figure 2. Microtubule regrowth after cold shock in wild-type and mutant cells. Anti-tubulin staining of fixed cells. Microtubules were depolymerized by a 30-min cold shock and then fixed at the indicated times after being returned to 32°C. Note that all mutants initially nucleate a single microtubule bundle, but *mto2*Δ mutants nucleate much faster and reach steady state more quickly than *mto1*Δ and *mto2*Δ *mto1*Δ mutants. The position of the nucleus in cells can be identified by faint negative staining. Bar, 2 μm.

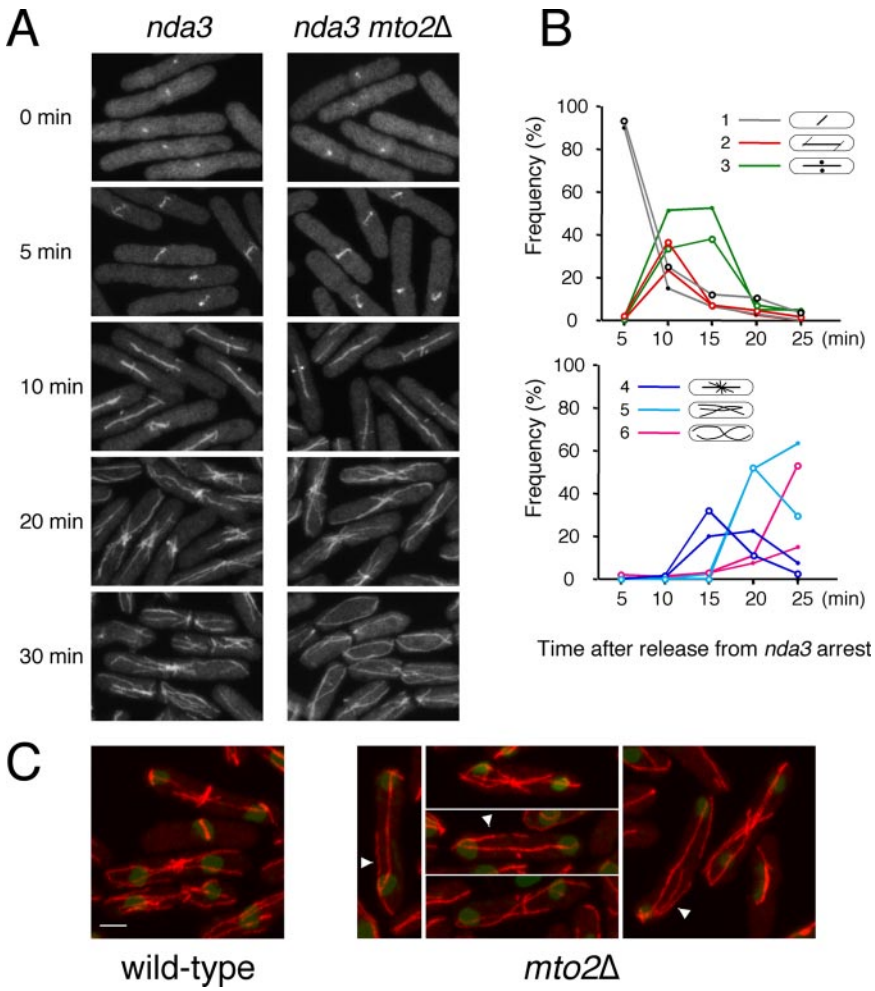

Figure 3. PAA formation of microtubules in *mto2*Δ mutants. Anti-tubulin staining of fixed cells. (A) Mitotic spindle, PAA, and interphase microtubule organization in wild-type and *mto2*Δ cells after release from *nda3* mitotic arrest. Note that spindles and PAAs occur at similar times in both strains, but *mto2*Δ mutants reach an interphase organization more quickly. (B) Quantitation of early (top) and late (bottom) microtubule structures at different times after release from the *nda3* arrest in the experiment in A. Filled circles, wild-type cells; open circles, *mto2*Δ. Early structures (classes 1–3) appear and disappear with comparable kinetics in the two strains, whereas well defined PAAs (class 4) are not sustained in *mto2*Δ mutants and are more quickly replaced by more disorganized microtubules (classes 5 and 6). (C) PAAs of microtubules in asynchronous wild-type and *mto2*Δ cells. Note aberrant PAA and cytoplasmic astral microtubules (arrowheads) in *mto2*Δ mutants. Bar, 2 μm.

ments after cold shock also were observed during live-cell imaging of *mto2*Δ cells expressing the GFP-tubulin fusion protein GFP-atb2 from the low-strength *nmt81* promoter. In contrast to wild-type cells, which nucleate microtubules from multiple independent sites (see Movie 01; Brunner and Nurse, 2000; Drummond and Cross, 2000; Tran *et al*., 2001; Sawin *et al*., 2004), *mto2*Δ mutants nucleated microtubules from only a single site on the nuclear surface, which we interpret to be the SPB (see Movies 02–05). *mto2*Δ mutants also contained fewer microtubule bundles, in particular when expressing GFP-atb2 from the medium-strength *nmt41* promoter (see Movie 05). In addition, microtubules in *mto2*Δ mutants displayed unusual dynamics not seen in wild-type cells, including bending around the cell tip and then sometimes breaking, generating a new microtubule bundle as a result (see Movies 02–05). Similar bend-breakage behavior has been observed previously in *mto1*Δ mutants (Sawin *et al*., 2004; see Discussion).

To investigate a role for *mto2*+ in mitotic microtubule nucleation, we examined microtubule regrowth after release from a mitotic metaphase arrest, by using the cold-sensitive β-tubulin mutant *nda3-km*311 (Hiraoka *et al*., 1984) in wild-type (i.e., *mto2*+) and *mto2*Δ backgrounds (Figure 3). Previous work showed that *mto1*Δ *nda3* mutants reassemble and elongate an intranuclear mitotic spindle at the same rate as *nda3* single mutants but are completely defective in the growth of cytoplasmic astral microtubules from the SPB and in the formation of a postanaphase array from the eMTOC at the end of mitosis (Sawin *et al*., 2004; Venkatram *et al*., 2004). By contrast, we found that under the same regime, *mto2*Δ *nda3* mutants were able to nucleate not only spindle microtubules but also cytoplasmic astral microtubules and PAA microtubules (Figure 3A). Interestingly, in these experiments the PAAs of *mto2*Δ *nda3* mutants seemed to be slightly less well focused than those of *nda3* single mutants and to reorganize slightly more rapidly (Figure 3B). We therefore investigated the organization of PAAs in asynchronous cultures. By immunofluorescence, we found that although PAAs were visible in actively cycling *mto2*Δ (i.e., *nda3*+) mutants, they varied widely in morphology and were often marked by fewer, longer microtubules, and mutant cells often contained long astral microtubules and/or additional microtubules not apparently focused at the eMTOC (Figure 3C).

To further understand the basis for this complexity, we followed the appearance of PAAs in live *mto2*Δ cells expressing *nmt81*:GFP-atb2 (see Movies 01–05). Although wild-type cells showed robust PAAs with continuous microtubule nucleation from eMTOCs (see Movie 01), *mto2*Δ mutants typically showed obvious but less frequent nucleation from the eMTOC, such that PAAs were either weak or highly transient. In addition, astral microtubules were clearly observed in *mto2*Δ mutants, and after nucleation, both PAA and astral microtubules were typically more stable dynamically, with astral microtubules often making long excursions into their sister cell before septation (see Movies 02–04). As with in-

terphase microtubule dynamics, these effects of *mto2*+ deletion seemed somewhat stronger in cells expressing *nmt41*:GFP-atb2 (see Movie 05). Collectively, these results suggest that, although mto2p is not absolutely required for PAA formation, it may nevertheless contribute to the stability of the eMTOC and PAA formation. The apparent stability of the PAA in *mto2*Δ *nda3* mutants may be a consequence of an extended mitotic arrest (see *Discussion*).

Together, the above-mentioned analyses of interphase and mitotic microtubule nucleation suggest that mto2p is involved in the regulation of microtubule nucleation in the same genetic network as mto1p and that mto2p is required for a specific subset of mto1p-dependent microtubule nucleation functions.

Localization of mto2p to Microtubule-organizing Centers

To determine the intracellular localization of mto2p, we tagged the carboxy-terminus of the endogenous *mto2*+ open reading frame with GFP, such that the resulting fusion protein is expressed from its endogenous promoter and is the sole source of mto2p in the cell (see, for example, Figure 6). In living cells, mto2-GFP was localized to the SPBs during both interphase and mitosis, to the eMTOC, and to satellite particles of varying intensity on cytoplasmic interphase microtubules (Figure 4A; see Movie 06). A similar localization has been previously observed for mto1-GFP, with mto1-GFP satellite particles showing rapid back-and-forth movements on microtubules (Sawin *et al*., 2004; Venkatram *et al*., 2004). Mto2-GFP satellites showed similar movements by time-lapse videomicroscopy, on both interphase and PAA microtubules (see Movie 07). Attempts to localize untagged mto2p in fixed cells with affinity-purified anti-mto2p antibodies (Figure 5) were unsuccessful, due to high cytoplasmic background (our unpublished data).

The similarity of mto2-GFP localization and movement to that of mto1-GFP suggested that the two proteins might colocalize. In live cells coexpressing mto2-CFP and mto1-YFP, we observed extensive colocalization of CFP and YFP signals at the SPB, at the cell division site and at interphase satellites (Figure 4B). These results suggest that mto2p and mto1p colocalize to MTOCs constitutively throughout the cell cycle.

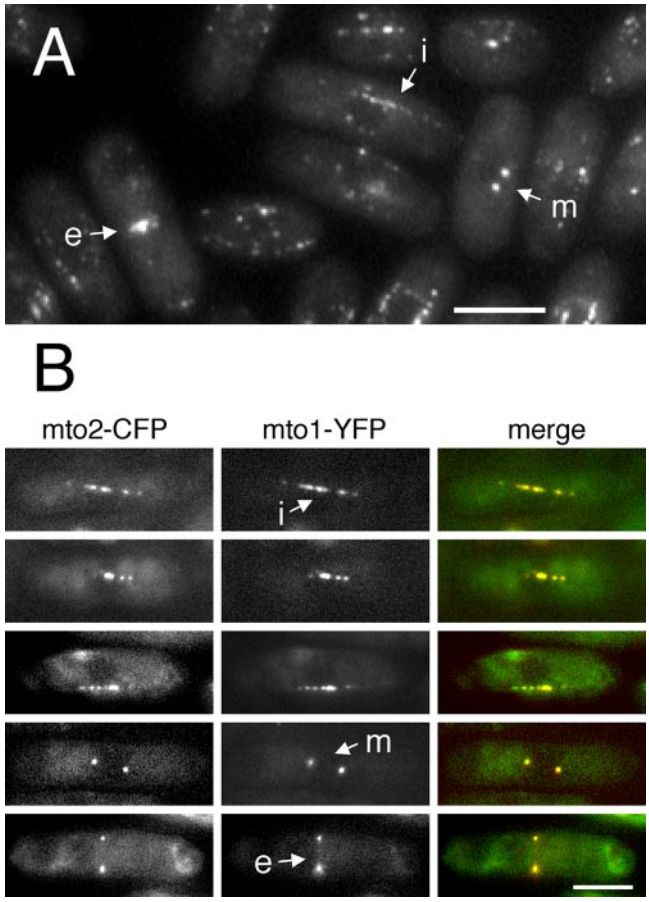

Figure 4. Mto2p localization in wild-type cells. (A) Mto2-GFP in live cells. Projection of Z-sections through the entire cell volume. Note localization to mitotic SPBs (arrow m) and eMTOC (arrow e) in mitotic and postmitotic cells, and satellite particles in interphase cells (arrow i). (B) Coexpression of mto2-CFP and mto1-YFP in live cells. Single Z-sections. The two signals colocalize during interphase (top three rows) as well as during mitosis (fourth row) and cell division (bottom row). Labeling convention as in A. Bars, 5 μm.

Mto2p Interacts Directly with mto1p

Given the colocalization of mto2p with mto1p at the light microscope level, we investigated whether mto2p and mto1p interact physically (Figure 5). We found that affinity-purified anti-mto2p antibodies were able to coimmunoprecipitate mto1p with mto2p in native fission yeast extracts (Figure 5A) and that anti-myc antibodies were able to coimmunoprecipitate mto2p with myc-tagged mto1p (Figure 5B). These results indicate that mto1p and mto2p are likely to exist in a common complex in vivo. To further define the regions of mto1 required for interaction with mto2p, we repeated coimmunoprecipitation experiments by using strains containing C-terminal truncations of myc-tagged mto1p. Both mto1(1-800)-myc and mto1(1-1051)-myc were able to coimmunoprecipitate mto2p, whereas mto1(1-285)-myc and mto1(1-500)-myc were not (Figure 5C). This suggests that a central portion of mto1p is likely to be important for its association with mto2p (full-length mto1p is 1115 amino acids; Figure 5E).

To determine whether the observed interaction between mto2p and mto1p is direct and to further map the regions of mto1p required for interaction with mto2p, we performed GST pull-down experiments by using bacterially expressed GST-mto2p and in vitro-translated mto1p. Initial experiments showed that GST-mto2p was able to pull down mto1(1-600), mto1(1-700), and mto1(1-800) but not mto1(1-500), suggesting that mto1p and mto2p bind directly and also that the GST pull-down experiments reproduced the nature of the interaction observed in our coimmunoprecipitation experiments (Figure 5D). A series of amino- and carboxyl-terminal deletions of in vitro-translated mto1p further showed that an ~90-amino acid sequence in the central portion of mto1p, between amino acids 461 and 549, is required for interaction with mto2p (Figure 5E; additional data not shown); this is distinct from the region of mto1p conserved among centrosomin-related proteins (mto1p amino acids 249–308).

Role of mto2p in mto1p Localization

Together with the physical association between mto2p and mto1p, the observation that *mto2*Δ mutants display only a subset of the microtubule nucleation defects seen in *mto1*Δ suggested that the association of mto2p with mto1p may be required to regulate specific aspects of mto1p function. We therefore investigated possible mechanisms by which mto2p might exert this effect.

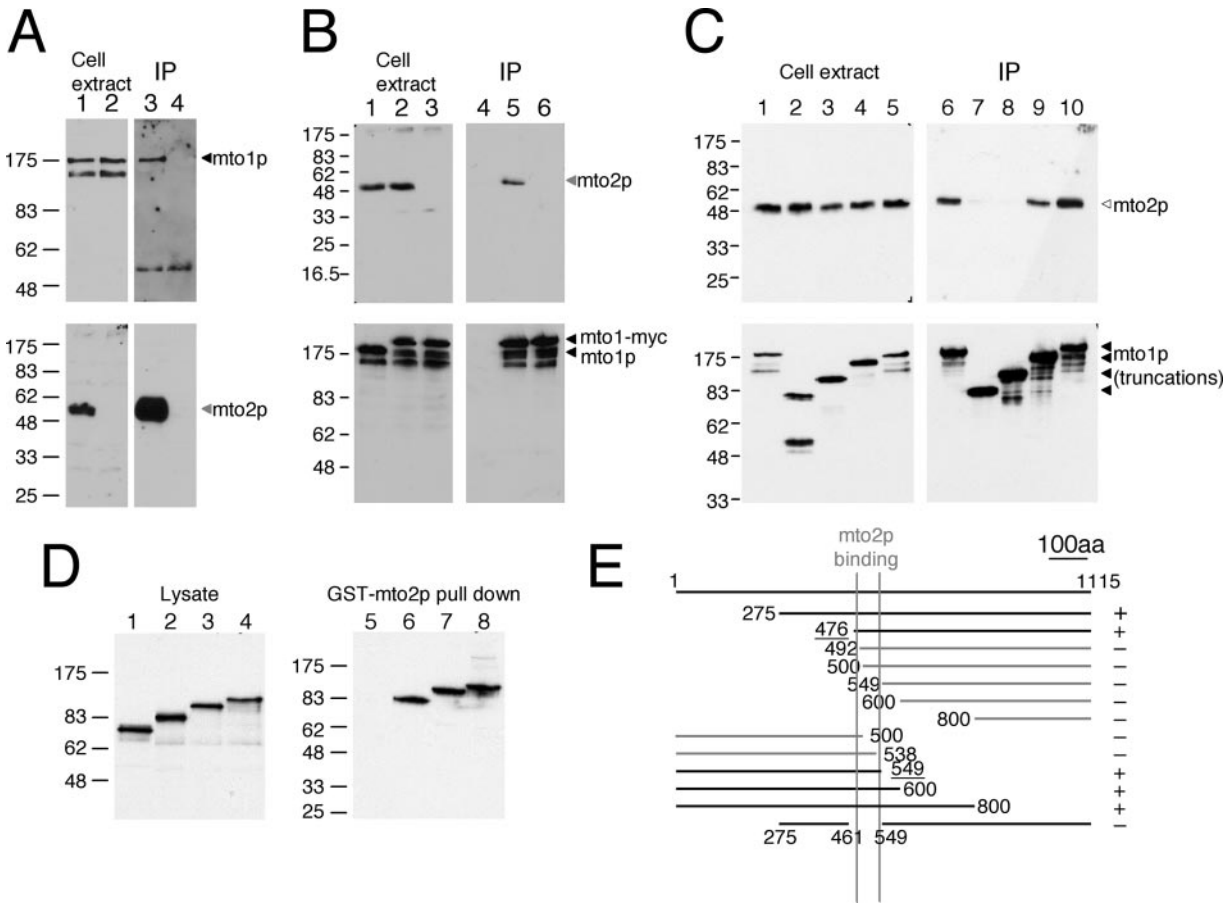

Figure 5. Physical interactions between mto2p and mto1p. (A) Immunoprecipitation of mto1p with mto2p from cell extracts. Affinity-purified anti-mto2p antibody was used for immunoprecipitation. Cell extracts and immunoprecipitates of wild-type (lanes 1 and 3) and *mto2*Δ (lanes 2 and 4) were blotted and probed with antibodies to mto1p (top) and mto2p (bottom). (B) Immunoprecipitation of mto2p with mto1-myc. Anti-myc antibody was used for immunoprecipitation. Cell extracts and immunoprecipitates of *mto1*+ (i.e., no tag on mto1p; lanes 1 and 4), *mto1-myc* (lanes 2 and 5), and *mto1-myc mto2*Δ (lanes 3 and 6) were blotted and probed with antibodies to mto2p (top) and mto1p (bottom). (C) Some truncated mto1 proteins cannot immunoprecipitate mto2p. Anti-myc antibody was used to immunoprecipitate carboxyl-terminal truncations of mto1-myc. Cell extracts and immunoprecipitates of full-length mto1-myc (1-1115; lanes 1 and 6), mto1(1-285)-myc (lanes 2 and 7), mto1(1-500)-myc (lanes 3 and 8), mto1(1-800)-myc (lanes 4 and 9), and mto1(1-1051)-myc (lanes 5 and 10) were blotted and probed with antibodies to mto2p (top) and mto1p (bottom). Immunoprecipitate lanes represent ~20× extract-equivalent loading relative to total cell extract lanes. (D) In vitro binding of mto1p truncations to GST-mto2p by pull-down assays. Mto1 proteins expressed in reticulocyte lysate (left) were tested for binding to GST-mto2 (right). Reticulocyte lysates and pull-downs of mto1(1-500) (lanes 1 and 5), mto1(1-600) (lanes 2 and 6), mto1(1-700) (lanes 3 and 7), and mto1(1-800) (lanes 4 and 8) were blotted and probed with antibodies to mto1p. (E) Summary of results of additional GST-mto2p pull-down assays, showing central region of mto1p required for binding to mto2p.

We first explored the possibility that mto1p protein levels might be altered in *mto2*Δ mutants, because interphase and PAA microtubule nucleation might be more sensitive than intranuclear spindle microtubule nucleation to mto1p levels. However, mto1p levels were not altered in *mto2*Δ mutants nor were mto2p levels altered in *mto1*Δ mutants (Figure 6).

Our previous work showed that during regrowth of interphase microtubules after cold shock, the nucleation from multiple sites around the cell nucleus that occurs in wild-type cells (Figure 2) is driven by a redistribution of mto1p to the nuclear surface, as a specific result of the cold treatment (Sawin *et al*., 2004). Because microtubule regrowth in *mto2*Δ mutants is restricted to the SPB in this assay, we examined mto1p localization upon cold-shock in *mto2*Δ mutants. Before cold-shock, anti-mto1p staining revealed mto1p at SPBs and eMTOCs in both wild-type and *mto2*Δ cells (Figure 7, A and B). Mto1p was also visible along microtubules in wild-type cells (Figure 7A; Sawin *et al*., 2004), although this was less apparent in *mto2*Δ cells (Figure 7B). On cold shock, in contrast

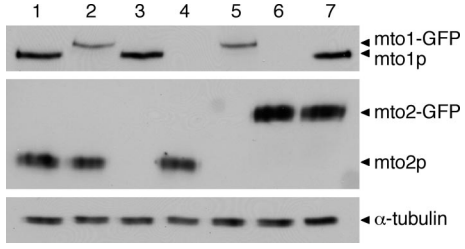

Figure 6. Mto1p and mto2p protein levels in wild-type and mutant strains. Extracts from wild-type cells (lane 1), as well as *mto1-GFP* (lane 2), *mto2*Δ (lane 3), *mto1*Δ (lane 4), *mto1-GFP mto2*Δ (lane 5), *mto2-GFP mto1*Δ (lane 6), and *mto2-GFP* (lane 7) were blotted and probed with antibodies to mto1p (top) and mto2p (middle). α-Tubulin also was probed, as a loading control (bottom). Note that deletion of mto2p does not affect mto1p levels, or vice-versa. Also note that GFP-tagging of mto1p slightly destabilizes the resulting fusion protein, whereas GFP-tagging of mto2p may slightly stabilize the resulting fusion.

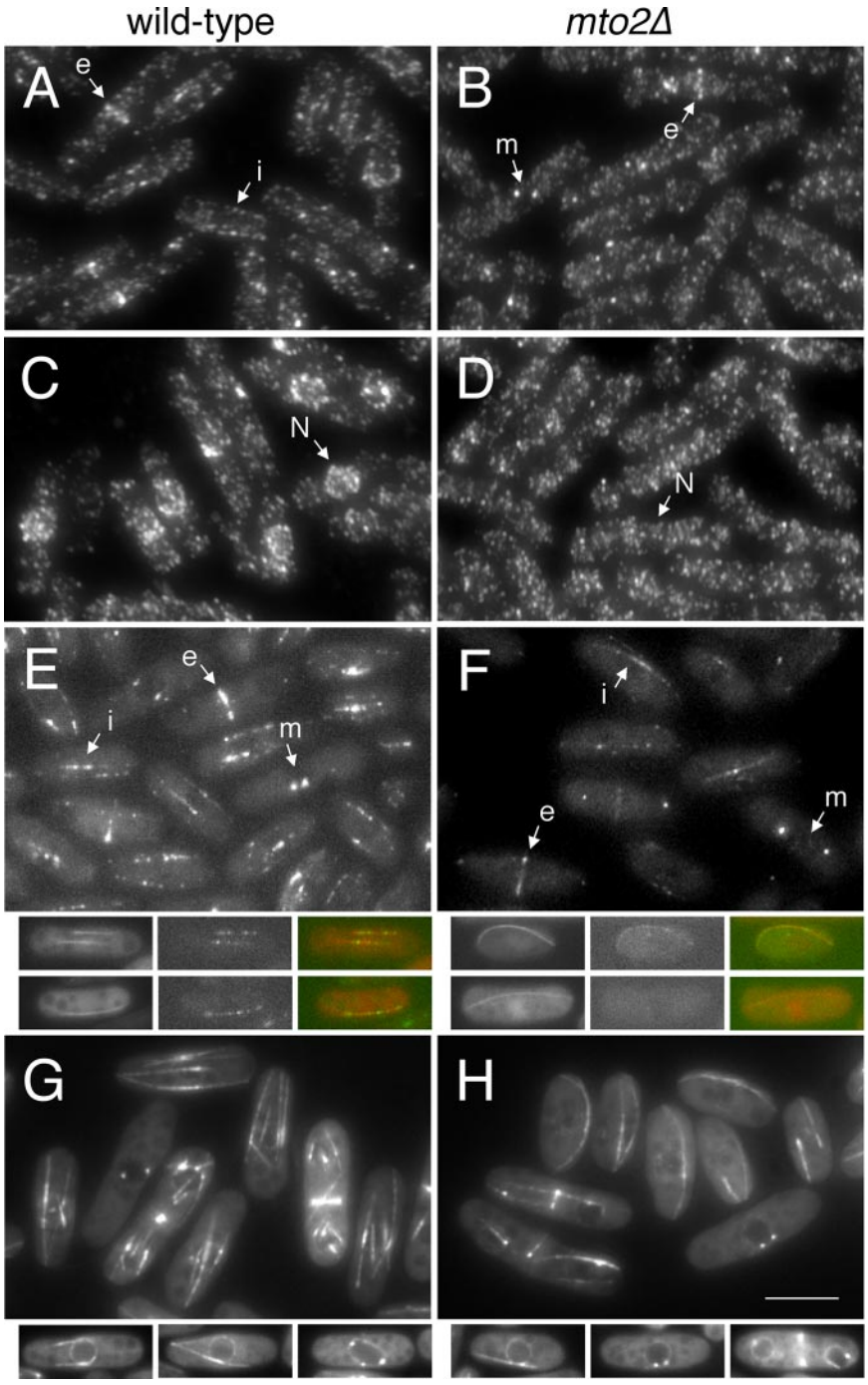

Figure 7. Mto1p localization in *mto2*Δ mutants. (A–D) Mto1p does not redistribute to the nuclear surface upon cold-shock in *mto2*Δ mutants. Immunofluorescent staining with affinity-purified anti-mto1p antibody. Wild-type and *mto2*Δ cells were fixed and stained (A and B) before and (C and D) after 30 min cold-shock at 0°C. Note interphase (i), mitotic SPB (m) and eMTOC (e) localization of mto1p. Nuclear position also is marked (N). (E and F) Localization of mto1-YFP in living wild-type and *mto2*Δ cells. Projections of Z-sections through the entire cell volume. Smaller panels show single Z-section examples of mto1-YFP in cells coexpressing CFP-atb2 tubulin. Note that not all microtubules in *mto2*Δ cells have associated mto1-YFP. Same labeling convention as above. (G and H) Localization of mildly overexpressed *nmt81*:GFP-mto1p in wild-type and *mto2*Δ cells. Projections of Z-sections through the entire cell volume. Small panels show examples of single Z-sections in interphase and mitotic cells, allowing visualization of the GFP-mto1p localized to the nuclear envelope that is obscured in projections. In all panels, images comparing wild-type and *mto2*Δ cells were always acquired and processed under identical conditions, allowing direct comparison of intensities. Bar, 5 μm (large panels); 7 μm (small panels).

to wild-type cells, no accumulation of mto1p was observed at the nuclear surface in *mto2*Δ mutants (Figure 7D), consistent with the *mto2*Δ microtubule nucleation phenotype. This suggested that deletion of *mto2*+ might affect the behavior of mto1p in vivo. We therefore further analyzed whether normal mto1p localization depended on mto2p.

Because mto1-GFP is localized to SPBs, eMTOCs, and dynamic microtubule-associated interphase satellites in living cells (Sawin *et al*., 2004), we sought to image mto1-GFP in *mto2*Δ mutants. Initial experiments suggested that mto1-GFP was at SPBs and eMTOCs in *mto2*Δ mutants, but cellular autofluorescence interfered with our ability to detect potentially faint mto1-GFP signals from interphase satellites (our unpublished data). We therefore focused our analysis on mto1-YFP localization, which is better separated spectrally from the autofluorescence (our unpublished data). In *mto2*Δ mutants, mto1-YFP was observed at SPBs and eMTOCs (Figure 7, E and F; see Movies 08 and 09), consistent with observed nucleation of cytoplasmic astral microtubules from the SPB and PAA microtubules from the eMTOC in *mto2*Δ mutants. However, mto1-YFP signal at eMTOCs was reduced in *mto2*Δ mutants relative to wild-type cells; this may contribute to the reduced PAA nucleation characteristic of *mto2*Δ mutants.

We also observed mto1-YFP interphase satellite particles in *mto2*Δ mutants, although relative to wild-type cells, the

mto1-YFP signal was faint and prone to photobleaching, and its localization to microtubules was more easily recognized in single sections than in projections encompassing the entire cell volume (compare Figure 7 with Movie 09). We confirmed this microtubule localization by coexpressing CFP-atb2 in double-label experiments (Figure 7, E and F); in some *mto2*Δ cells, microtubules without associated mto1-YFP were seen (compare also Movies 08 and 09). Under optimal imaging conditions, we observed dynamic movement of mto1-YFP interphase satellites on microtubules in *mto2*Δ mutants, although this was difficult to detect routinely and was not easily seen in all cells (Movies 10 and 11).

We also examined the localization of moderately overexpressed GFP-mto1p in wild-type and *mto2*Δ strains (Figure 7, G and H). Expressed at three to four times wild-type levels from the *nmt81* promoter (our unpublished data), GFP-mto1p showed localization to the SPB and eMTOC, as well as noticeable localization to the nuclear envelope (Figure 7G) and apparently uniform decoration of cytoplasmic microtubules, in contrast to the satellite-particle localization observed when mto1-GFP is expressed from its endogenous promoter. Interestingly, none of these localizations required the presence of mto2p (Figure 7H).

Together, the above-mentioned results indicate that mto2p is not absolutely required for localization of mto1p to the SPB or to eMTOCs or for localization to interphase cytoplasmic microtubules; however, the degree to which mto1p localizes to eMTOCs and interphase microtubules does seem to depend partially on mto2p. Moreover, in the cold shock assay, relocalization of mto1p to the nuclear surface depends on mto2p. These results suggest that although mto2p may affect some aspects of mto1p localization under specific experimental conditions, this is unlikely to be the sole cause of all of the observed microtubule nucleation defects in *mto2*Δ mutants (see *Discussion* for further details).

Mto2p Is Required for Coimmunoprecipitation of the γ-Tubulin Complex with mto1p and for Proper In Vivo Localization of the γ-Tubulin Complex

Because the major molecular role for mto1p in microtubule nucleation seems to be to bind and recruit the γ-tubulin complex to different MTOCs (Sawin *et al*., 2004; Venkatram *et al*., 2004), we tested whether mto1p could still bind to the γ-tubulin complex in the absence of mto2p. Strikingly, whereas cytoplasmic extracts prepared from cells expressing mto1-myc could coimmunoprecipitate mto2p, γ-tubulin, and hemagglutinin (HA)-tagged alp4p (an essential component of the γ-tubulin complex; Vardy and Toda, 2000) with mto1-myc, neither γ-tubulin nor alp4-HA was coimmunoprecipitated with mto1-myc to any extent in *mto2*Δ cells, even after very long exposures of Western blots (Figure 8; additional data not shown). This indicates that soluble forms of mto1p are not associated with the γ-tubulin complex in *mto2*Δ mutants; we address this further below in relation to *mto1*Δ and *mto2*Δ phenotypes (see *Discussion*).

As a corollary to the coimmunoprecipitation experiments, we examined the localization of GFP-tagged alp4p in wild-type and *mto2*Δ cells in vivo. In wild-type cells, alp4-GFP was found at SPBs throughout the cell cycle, at eMTOCs at the end of mitosis, and on microtubule-associated satellite particles during interphase (Vardy and Toda, 2000; Zimmerman *et al*., 2004a; Figure 9A). By contrast, in *mto2*Δ cells, alp4-GFP interphase satellite particles were not observed, and only barely detectable amounts of alp4-GFP were seen at eMTOCs, although alp4-GFP remained associated with SPBs throughout the cell cycle (Figure 9B). These results indicate that mto2p is required for the correct cytoplasmic

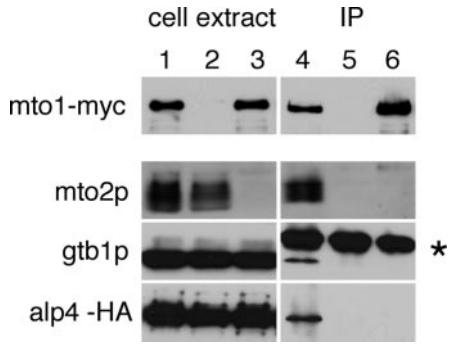

Figure 8. The γ-tubulin complex is no longer coimmunoprecipitated with mto1p in *mto2*Δ cells. Anti-myc antibody was used for immunoprecipitation. Cell extracts and immunoprecipitates of *mto1-myc alp4-HA* (lanes 1 and 4), negative control *mto1+ alp4-HA* (i.e., no tag on mto1p; lanes 2 and 5), and *mto1-myc alp4-HA mto2*Δ (lanes 3 and 6) were blotted and probed with antibodies to myc (top), mto2p (second), γ-tubulin (third), and HA (bottom). Asterisk marks the position of anti-myc IgG heavy chain in immunoprecipitates; γ-tubulin is the band underneath. Immunoprecipitate lanes represent ~40× extract equivalent loading relative to total cell extract lanes.

localization of the γ-tubulin complex at non-SPB sites; in conjunction with our immunoprecipitation data, this provides a straightforward mechanistic explanation for the range of microtubule nucleation defects observed in *mto2*Δ mutants.

Mto1p Is Required for mto2p Localization

We also examined mto2-GFP localization in *mto1*Δ mutants. Strikingly, mto2-GFP interphase satellites were no longer observed in *mto1*Δ cells, and mto2-GFP localization to SPBs and eMTOCs was almost abolished (Figure 10B). Approximately one-third of cells showed a faint GFP signal suggestive of the SPB, and dividing cells showed only a very faint signal at the septum, or no signal at all. The faint signals were always small and punctate rather than band-like (compare Figure 10, A and B), suggesting that this small amount of mto2-GFP might be recruited to the division site only at the very end of septation; alternatively, it is possible that low amounts of mto2-GFP are present throughout septation in *mto1*Δ mutants but are visible only when concentrated into

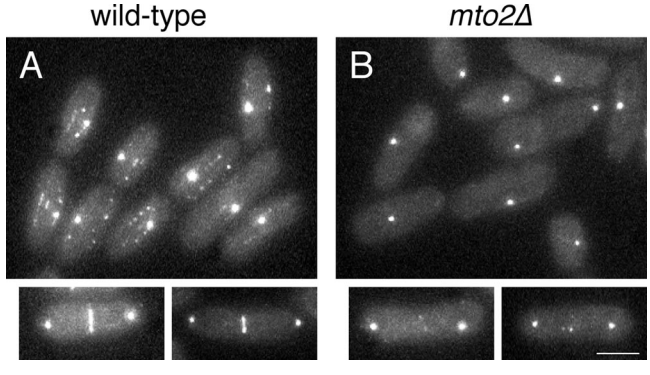

Figure 9. The γ-tubulin complex is not properly localized to eMTOCs or interphase satellite particles in *mto2*Δ mutants. Alp4-GFP localization in live wild-type (A) and *mto2*Δ mutant (B) cells. Large panels show interphase cells (with one just-divided cell pair in B); small panels show dividing cells. Bar, 5 μm.

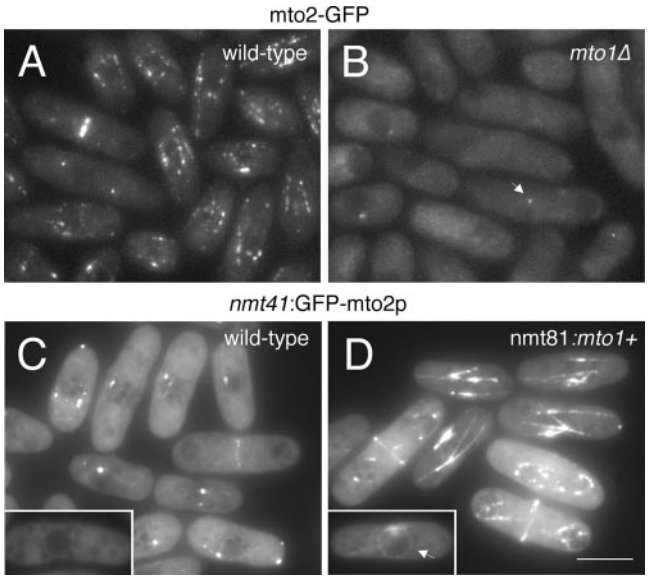

Figure 10. Mto1p is required for mto2p localization. (A and B) Localization of mto2-GFP in live wild-type (A) and *mto1*Δ (B) cells. Projections of Z-sections through the entire cell volume. Images in A and B were acquired and processed under identical conditions, allowing direct comparison of intensities. (C and D) Localization of overexpressed *nmt41*:GFP-mto2p in wild-type cells (C) and cells mildly overexpressing *nmt81*:mto1+ (i.e., untagged mto1p) (D). Projections of Z-sections through the entire cell volume. Smaller panels show single Z-section examples of *nmt41*:GFP-mto2p localizing to the nuclear envelope only when mto1p is overexpressed (arrow). Images in C and D were acquired and processed under identical conditions, allowing direct comparison of intensities. Bar, 5 μm.

a small volume. Because mto1p and mto2p interact, we tried to test more directly whether mto2p localization to microtubules occurs specifically via its interaction with mto1p. We found that in *mto1*+ cells, overexpressed GFP-mto2p (*nmt41*:GFP-mto2p) was easily visualized at SPBs and at eMTOCs but was not seen on microtubules above levels of cytoplasmic GFP-mto2p background fluorescence; some protein aggregation also was observed (Figure 10C). However, when *nmt81*:mto1p was simultaneously overexpressed in the GFP-mto2p–overexpressing cells, GFP-mto2p now localized to interphase microtubules, as well as to the nuclear envelope, mirroring the localization of *nmt81*:GFP-mto1p (Figure 10D; compare with Figure 7G). These results indicate not only that mto1p is required for normal mto2p localization to most subcellular structures but also that mto1p protein levels are limiting for mto2p localization, suggesting that mto2p localization to microtubules occurs in the form of a mto1p/mto2p protein complex in which mto1p provides the microtubule targeting.

DISCUSSION

Model for mto2p Function

In this work, we have identified and characterized a novel protein, mto2p, which plays an important role in the regulation of fission yeast microtubule nucleation. Most microtubule nucleation in eukaryotic cells is thought to be mediated by the γ-tubulin complex (Gunawardane *et al*., 2000; Oakley, 2000; Schiebel, 2000; Job *et al*., 2003). In fission yeast, normal cytoplasmic microtubule nucleation from the SPB, eMTOC, and iMTOCs requires the centrosomin-related protein mto1p to recruit the γ-tubulin complex to these MTOCs (Sawin *et al*., 2004; Venkatram *et al*., 2004). Given the spatiotemporal diversity of fission yeast MTOCs (Hagan, 1998; Drummond and Cross, 2000; Tran *et al*., 2001; Sawin *et al*., 2004; Venkatram *et al*., 2004; Zimmerman *et al*., 2004a), it might be expected that regulators of mto1p exist within cells. Here, we have shown that mto2p is required for cytoplasmic microtubule nucleation from iMTOCs but not from the SPB. Mto2p also contributes significantly to eMTOC nucleation. In conjunction with our biochemical and localization studies, these data suggest a provisional model in which mto2p regulates microtubule nucleation mediated by mto1p and the γ-tubulin complex. We propose the following four main points, which are discussed in more detail below: 1) Mto2p is a stable component of an mto1p-containing protein complex that recruits the γ-tubulin complex to MTOCs. 2) Mto1p interphase satellite particles, which may represent the soluble population of mto1p complexes that can be probed by immunoprecipitation, do not bind the γ-tubulin complex in the absence of mto2p. 3) Mto1p complexes at SPBs and eMTOCs, which may not be identifiable in immunoprecipitation experiments because they are largely insoluble, can associate with the γ-tubulin complex even in the absence of mto2p. 4) Mto2p is not required for the general ability of the mto1p complex to be targeted to SPB, eMTOC, and interphase satellite iMTOCs but may contribute to the efficient recruitment of mto1p to the eMTOC and the behavior and/or dynamics of mto1p satellites.

With regard to the first point, we have shown that mto1p and mto2p are very closely colocalized at MTOCs throughout the cell cycle and that mto2p is likely to bind directly to a central portion of mto1p. In addition, mto2p is coimmunoprecipitated with mto1-myc much more efficiently than the γ-tubulin complex (Figure 8). This suggests to us that it may be most appropriate to think of γ-tubulin complex recruitment to MTOCs as involving an interaction between the γ-tubulin complex and an mto1p/mto2p complex.

The second two points of the model raise several related issues concerning protein–protein interactions between mto1p and the γ-tubulin complex. The γ-tubulin complex is no longer found in mto1-myc immunoprecipitates from cytoplasmic extracts in *mto2*Δ strains. This could be interpreted to mean that in this instance, absolutely no mto1p in the cell is capable of interacting with the γ-tubulin complex. However, our current understanding of the role of γ-tubulin in fission yeast microtubule nucleation (Horio *et al*., 1991; Stearns *et al*., 1991; Paluh *et al*., 2000; Vardy and Toda, 2000; Heitz *et al*., 2001; Fujita *et al*., 2002; Zimmerman *et al*., 2004a) and previous and current analyses of *mto1*Δ and *mto2*Δ mutant phenotypes (Sawin *et al*., 2004; Venkatram *et al*., 2004) lead us to suggest that small amounts of solid-phase mto1p interacting with the γ-tubulin complex at SPBs and eMTOCs may be sufficient for the nucleation activities observed in cells. This view is supported by our observation of extremely low levels of alp4-GFP at eMTOCs in *mto2*Δ mutants, which correlates with their reduced microtubule nucleation activity. In general, essentially all biochemical work on γ-tubulin in eukaryotes has been done on soluble complexes, and very little is known about solid-phase γ-tubulin complexes in eukaryotes (see, for example, Salas, 1999; Terada *et al*., 2003; Zimmerman *et al*., 2004b).

A second issue concerns the role of mto2p in promoting association of mto1p with the γ-tubulin complex. One possibility is that mto2p forms a "bridge" between an mto1p/mto2p complex and the γ-tubulin complex. If this were the case, we might expect a functional analog of mto2p to be

similarly associated with mto1p at SPBs and eMTOCs, in the place of mto2p. Although this has not yet been investigated, we note that mto2p seems to remain associated with mto1p at all MTOCs, throughout the cell cycle (even when, in our view, it may not be very important for mto1p function). Thus, we speculate that the role of mto2p in promoting γ-tubulin complex binding to mto1p may be more indirect, possibly allosteric, and that supplementary mechanisms may promote mto2p-independent γ-tubulin complex binding to mto1p at SPBs and eMTOCs. Future experiments to dissect the molecular interactions governing localization of mto1p and γ-tubulin complex association will help to resolve this issue.

The final point of the model concerns targeting of an mto1p/mto2p complex to MTOCs and its consequences for nucleation. Overall, our data from GFP and YFP fusion proteins suggest that mto1p targeting is independent of mto2p and that mto2p targeting depends on mto1p. However, in the two cases where *mto2*Δ microtubule nucleation is not completely normal (i.e., iMTOC and eMTOC nucleation), levels of mto1-YFP are somewhat reduced and/or more difficult to detect at the corresponding MTOCs. This could be due to unrecognized defects in the mto1p complex itself or alternatively to the defects in microtubule organization known to exist in *mto2*Δ mutants. Aberrantly organized microtubules might fail to provide an optimal distribution of tracks or loading sites for mto1p complexes (for example, in the form of microtubule minus ends). In either case, it is worth noting that achieving a full complement of mto1p at eMTOCs could depend on microtubule-based movement of mto1p on PAA microtubules, which are themselves abnormal in *mto2*Δ mutants. Further work toward understanding the nature of satellite particle movements, particularly using in vitro systems, will help to clarify these issues.

Complicating our understanding of the role of mto2p in the subcellular targeting of mto1p is the fact that mto1p does not redistribute properly to the nuclear surface in cold shock experiments in *mto2*Δ mutants. This result stands in apparent opposition to our observations with GFP- and YFP-fusions to mto1p in live *mto2*Δ cells, especially with regard to *nmt81*:GFP-mto1p localization, for reasons which remain unclear. The fact that a significant fraction of mto1p may not remain in situ after fixation (Sawin *et al*., 2004) may be a contributory factor. In any case, the microtubule nucleation defects seen in *mto2*Δ mutants both in the cold shock experiment and during live cell analysis are most easily understood by the failure of cytoplasmic mto1p complexes to associate with the γ-tubulin complex, as shown in our immunoprecipitation and alp4-GFP localization studies.

Microtubule Nucleation and Dynamics in mto2Δ *Mutants*

Under steady-state growth conditions, *mto1*Δ mutants do not nucleate new interphase microtubules, and during recovery from cold shock they nucleate microtubules very poorly, and only from the SPB (Sawin *et al*., 2004; Venkatram *et al*., 2004). By contrast, *mto2*Δ cells efficiently nucleate interphase microtubules both during steady-state growth and after cold shock, but in both cases apparently only from the SPB. How do we account for these different microtubule nucleation phenotypes relative to each other and to wild-type cells? In fission yeast, the discoid SPB is associated with the nuclear envelope (Ding *et al*., 1997). It has been proposed previously that mto1p might be localized to the cytoplasmic face of the SPB in wild-type cells and that the poor SPB-mediated microtubule nucleation seen in *mto1*Δ mutants after cold shock may be driven by an mto1p paralog, pcp1p, from the nucleoplasmic face of the SPB (Sawin *et al*., 2004; Venkatram *et al*., 2004). We suggest that the efficient nucleation of cytoplasmic microtubules from the SPB in *mto2*Δ mutants is driven not by pcp1p but by active mto1p localized to the cytoplasmic face of the SPB. This mto2p-independent localization of mto1p also would account for the nucleation of cytoplasmic astral microtubules seen during mitosis in *mto2*Δ mutants and not *mto1*Δ mutants. In wild-type (i.e., *mto2*+) interphase cells, the additional ability to recruit the γ-tubulin complex to mto1p satellites would drive non-SPB–mediated microtubule nucleation.

At the end of mitosis in asynchronous cultures, *mto1*Δ mutants completely fail to form a PAA (Sawin *et al*., 2004; Venkatram *et al*., 2004), whereas *mto2*Δ mutants nucleate PAA microtubules but at a reduced frequency relative to wild-type cells. This can be explained by the presence of active mto1p at eMTOCs in *mto2*Δ mutants, but at a reduced level (see comments above). In contrast, after release from an *nda3* mitotic arrest, *mto2*Δ cells show a more robust PAA, similar to wild-type cells. To explain this, we suggest that during an extended mitotic arrest in *nda3 mto2*Δ mutants, additional mto1p may be able to slowly accumulate at the cell division site. The mechanism of mto1p targeting to the division site is not known but may involve an interaction with the cytokinetic actin ring (Heitz *et al*., 2001; Pardo and Nurse, 2003; Sawin *et al*., 2004), which is formed and maintained during the *nda3* arrest (Chang *et al*., 1996).

Finally, we note that the dynamics of interphase, PAA, and astral microtubules in *mto2*Δ mutants are different from wild-type cells. In particular, *mto2*Δ interphase microtubule dynamics look like those in *mto1*Δ cells, with abnormally bundled microtubules curling around cell tips and bend-breakage events generating new microtubule fragments (Sawin *et al*., 2004). We have previously suggested for *mto1*Δ mutants that these phenomena may represent an indirect consequence of altering the number of microtubule nucleation sites in a system with a fixed volume and tubulin concentration (see Sawin *et al*., 2004 for a further discussion). We believe an identical case can be made for *mto2*Δ mutants. Although we will not repeat the detailed arguments here, we note that theoretical calculations based on a simplified model of dynamic instability in a closed system arrive at conclusions consistent with this view (Mitchison and Kirschner, 1987).

ACKNOWLEDGMENTS

We thank A. Douglas and P. Sasajala for contributions to this work during summer projects; F. Chang, K. Gull, I. Stancheva, and T. Toda for antibodies, strains, and plasmids; H. Ohkura for comments and discussion; and K. Gould, S. Venkatram, and P. Tran for alerting us to similar work on mto2p in the respective laboratories. K.E.S. is a Wellcome Trust Senior Research Fellow in Basic Biomedical Sciences. H.A.S. is a Caledonian Research Fellow. This work was supported by the Wellcome Trust.

REFERENCES

Alfa, C., Fantes, P., Hymas, J., McLeod, M., and Warbrick, E. (1993). Experiments with Fission Yeast: A Laboratory Course Manual, Cold Spring Harbor, NY: Cold Spring Harbor Laboratory Press.

Andersen, J. S., Wilkinson, C. J., Mayor, T., Mortensen, P., Nigg, E. A., and Mann, M. (2003). Proteomic characterization of the human centrosome by protein correlation profiling. Nature *426*, 570–574.

Bahler, J., Wu, J. Q., Longtine, M. S., Shah, N. G., McKenzie, A., 3rd, Steever, A. B., Wach, A., Philippsen, P., and Pringle, J. R. (1998). Heterologous modules for efficient and versatile PCR-based gene targeting in Schizosaccharomyces pombe. Yeast *14*, 943–951.

Brunner, D., and Nurse, P. (2000). CLIP170-like tip1p spatially organizes microtubular dynamics in fission yeast. Cell *102*, 695–704.

Chang, F., Woollard, A., and Nurse, P. (1996). Isolation and characterization of fission yeast mutants defective in the assembly and placement of the contractile actin ring. J. Cell Sci. *109*, 131–142.

Ching, Y. P., Qi, Z., and Wang, J. H. (2000). Cloning of three novel neuronal Cdk5 activator binding proteins. Gene *242*, 285–294.

Ding, R., West, R. R., Morphew, D. M., Oakley, B. R., and McIntosh, J. R. (1997). The spindle pole body of Schizosaccharomyces pombe enters and leaves the nuclear envelope as the cell cycle proceeds. Mol. Biol. Cell *8*, 1461–1479.

Drummond, D. R., and Cross, R. A. (2000). Dynamics of interphase microtubules in Schizosaccharomyces pombe. Curr. Biol. *10*, 766–775.

Evan, G. I., Lewis, G. K., Ramsay, G., and Bishop, J. M. (1985). Isolation of monoclonal antibodies specific for human c-myc proto-oncogene product. Mol. Cell. Biol. *5*, 3610–3616.

Flory, M. R., Morphew, M., Joseph, J. D., Means, A. R., and Davis, T. N. (2002). Pcp1p, an Spc110p-related calmodulin target at the centrosome of the fission yeast *Schizosaccharomyces pombe*. Cell Growth Differ. *13*, 47–58.

Fujita, A., Vardy, L., Garcia, M. A., and Toda, T. (2002). A fourth component of the fission yeast gamma-tubulin complex, Alp16, is required for cytoplasmic microtubule integrity and becomes indispensable when gamma-tubulin function is compromised. Mol. Biol. Cell *13*, 2360–2373.

Gachet, Y., Tournier, S., Millar, J. B., and Hyams, J. S. (2001). A MAP kinase-dependent actin checkpoint ensures proper spindle orientation in fission yeast. Nature *412*, 352–355.

Gachet, Y., Tournier, S., Millar, J. B., and Hyams, J. S. (2004). Mechanism controlling perpendicular alignment of the spindle to the axis of cell division in fission yeast. EMBO J. *23*, 1289–1300.

Glynn, J. M., Lustig, R. J., Berlin, A., and Chang, F. (2001). Role of bud6p and tea1p in the interaction between actin and microtubules for the establishment of cell polarity in fission yeast. Curr. Biol. *11*, 836–845.

Gunawardane, R. N., Lizarraga, S. B., Wiese, C., Wilde, A., and Zheng, Y. (2000). gamma-Tubulin complexes and their role in microtubule nucleation. Curr. Top. Dev. Biol. *49*, 55–73.

Hagan, I. M. (1998). The fission yeast microtubule cytoskeleton. J. Cell Sci. *111*, 1603–1612.

Heitz, M. J., Petersen, J., Valovin, S., and Hagan, I. M. (2001). MTOC formation during mitotic exit in fission yeast. J. Cell Sci. *114*, 4521–4532.

Hiraoka, Y., Toda, T., and Yanagida, M. (1984). The NDA3 gene of fission yeast encodes beta-tubulin: a cold-sensitive nda3 mutation reversibly blocks spindle formation and chromosome movement in mitosis. Cell *39*, 349–358.

Horio, T., Uzawa, S., Jung, M. K., Oakley, B. R., Tanaka, K., and Yanagida, M. (1991). The fission yeast gamma-tubulin is essential for mitosis and is localized at microtubule organizing centers. J. Cell Sci. *99*, 693–700.

Job, D., Valiron, O., and Oakley, B. (2003). Microtubule nucleation. Curr. Opin. Cell Biol. *15*, 111–117.

Kawaguchi, S., and Zheng, Y. (2004). Characterization of a *Drosophila* centrosome protein CP309 that shares homology with Kendrin and CG-NAP. Mol. Biol. Cell *15*, 37–45.

Knop, M., and Schiebel, E. (1998). Receptors determine the cellular localization of a gamma-tubulin complex and thereby the site of microtubule formation. EMBO J. *17*, 3952–3967.

Megraw, T. L., Li, K., Kao, L. R., and Kaufman, T. C. (1999). The centrosomin protein is required for centrosome assembly and function during cleavage in *Drosophila*. Development *126*, 2829–2839.

Mitchison, T. J., and Kirschner, M. W. (1987). Some thoughts on the partitioning of tubulin between monomer and polymer under conditions of dynamic instability. Cell Biophys. *11*, 35–55.

Moreno, S., Klar, A., and Nurse, P. (1991). Molecular analysis of the fission yeast *Schizosaccharomyces pombe*. Methods Enzymol. *194*, 795–823.

Oakley, B. R. (2000). gamma-Tubulin. Curr. Top. Dev. Biol. *49*, 27–54.

Oliferenko, S., and Balasubramanian, M. K. (2002). Astral microtubules monitor metaphase spindle alignment in fission yeast. Nat. Cell Biol. *4*, 816–820.

Paluh, J. L., Nogales, E., Oakley, B. R., McDonald, K., Pidoux, A. L., and Cande, W. Z. (2000). A mutation in gamma-tubulin alters microtubule dynamics and organization and is synthetically lethal with the kinesin-like protein pkl1p. Mol. Biol. Cell *11*, 1225–1239.

Pardo, M., and Nurse, P. (2003). Equatorial retention of the contractile actin ring by microtubules during cytokinesis. Science *300*, 1569–1574.

Rios, R. M., Sanchis, A., Tassin, A. M., Fedriani, C., and Bornens, M. (2004). GMAP-210 recruits gamma-tubulin complexes to cis-Golgi membranes and is required for Golgi ribbon formation. Cell *118*, 323–335.

Salas, P. J. (1999). Insoluble gamma-tubulin-containing structures are anchored to the apical network of intermediate filaments in polarized CACO-2 epithelial cells. J. Cell Biol. *146*, 645–658.

Sawin, K. E., Lourenco, P. C., and Snaith, H. A. (2004). Microtubule nucleation at non-spindle pole body microtubule-organizing centers requires fission yeast centrosomin-related protein mod20p. Curr. Biol. *14*, 763–775.

Sawin, K. E., Mitchison, T. J., and Wordeman, L. G. (1992). Evidence for kinesin-related proteins in the mitotic apparatus using peptide antibodies. J. Cell Sci. *101*, 303–313.

Sawin, K. E., and Nurse, P. (1998). Regulation of cell polarity by microtubules in fission yeast. J. Cell Biol. *142*, 457–471.

Sawin, K. E., and Snaith, H. A. (2004). Role of microtubules and tea1p in establishment and maintenance of fission yeast cell polarity. J. Cell Sci. *117*, 689–700.

Schiebel, E. (2000). gamma-Tubulin complexes: binding to the centrosome, regulation and microtubule nucleation. Curr. Opin. Cell Biol. *12*, 113–118.

Snaith, H. A., and Sawin, K. E. (2003). Fission yeast mod5p regulates polarized growth through anchoring of tea1p at cell tips. Nature *423*, 647–651.

Stearns, T., Evans, L., and Kirschner, M. (1991). Gamma-tubulin is a highly conserved component of the centrosome. Cell *65*, 825–836.

Stearns, T., and Kirschner, M. (1994). In vitro reconstitution of centrosome assembly and function: the central role of gamma-tubulin. Cell *76*, 623–637.

Suelmann, R., Sievers, N., Galetzka, D., Robertson, L., Timberlake, W. E., and Fischer, R. (1998). Increased nuclear traffic chaos in hyphae of *Aspergillus nidulans*: molecular characterization of apsB and in vivo observation of nuclear behaviour. Mol. Microbiol. *30*, 831–842.

Takahashi, M., Yamagiwa, A., Nishimura, T., Mukai, H., and Ono, Y. (2002). Centrosomal proteins CG-NAP and Kendrin provide microtubule nucleation sites by anchoring gamma-tubulin ring complex. Mol. Biol. Cell *13*, 3235–3245.

Terada, Y., Uetake, Y., and Kuriyama, R. (2003). Interaction of Aurora-A and centrosomin at the microtubule-nucleating site in *Drosophila* and mammalian cells. J. Cell Biol. *162*, 757–763.

Thompson, H. M., Cao, H., Chen, J., Euteneuer, U., and McNiven, M. A. (2004). Dynamin 2 binds gamma-tubulin and participates in centrosome cohesion. Nat. Cell Biol. *6*, 335–342.

Tran, P. T., Marsh, L., Doye, V., Inoue, S., and Chang, F. (2001). A mechanism for nuclear positioning in fission yeast based on microtubule pushing. J. Cell Biol. *153*, 397–411.

Vardy, L., and Toda, T. (2000). The fission yeast gamma-tubulin complex is required in G(1) phase and is a component of the spindle assembly checkpoint. EMBO J. *19*, 6098–6111.

Venkatram, S., Tasto, J. J., Feoktistova, A., Jennings, J. L., Link, A. J., and Gould, K. L. (2004). Identification and characterization of two novel proteins affecting fission yeast gamma-tubulin complex function. Mol. Biol. Cell *15*, 2287–2301.

Verde, I., Pahlke, G., Salanova, M., Zhang, G., Wang, S., Coletti, D., Onuffer, J., Jin, S. L., and Conti, M. (2001). Myomegalin is a novel protein of the Golgi/centrosome that interacts with a cyclic nucleotide phosphodiesterase. J. Biol. Chem. *276*, 11189–11198.

Woods, A., Sherwin, T., Sasse, R., MacRae, T. H., Baines, A. J., and Gull, K. (1989). Definition of individual components within the cytoskeleton of *Trypanosoma brucei* by a library of monoclonal antibodies. J. Cell Sci. *93*, 491–500.

Zheng, Y., Wong, M. L., Alberts, B., and Mitchison, T. (1995). Nucleation of microtubule assembly by a gamma-tubulin-containing ring complex. Nature *378*, 578–583.

Zimmerman, S., Tran, P. T., Daga, R. R., Niwa, O., and Chang, F. (2004a). Rsp1p, a J domain protein required for disassembly and assembly of microtubule organizing centers during the fission yeast cell cycle. Dev. Cell *6*, 497–509.

Zimmerman, W. C., Sillibourne, J., Rosa, J., and Doxsey, S. J. (2004b). Mitosis-specific anchoring of gamma tubulin complexes by pericentrin controls spindle organization and mitotic entry. Mol. Biol. Cell *15*, 3642–3657.